

TOMOGRAPHIC IMAGING OF FLUID MIXING IN 3-D FOR SINGLE-FEED SEMI-BATCH OPERATION OF A STIRRED VESSEL

S. J. Stanley¹, R. Mann¹ and K. Primrose²

¹Department of Chemical Engineering, UMIST, PO Box 88, Manchester, England, M60 1QD

²Industrial Tomography Systems, 47 Newton Street, Manchester, England, M1 1FT

With fast data acquisition and good spatial discrimination, electrical resistance tomography (ERT) provides a non-invasive and non-intrusive technique to interrogate, in 3-D, the concentration fields inside a typical stirred vessel. A newly refurbished vertically assembled 16-sensor 8-ring electrode array has been used to image the full volume of a 2,300 litre pilot scale vessel for single-feed semi-batch operation. Images reconstructed from the raw ERT data are represented firstly as pixel conductivity distributions and secondly as time incremented 3-D solid-body colour-scaled isosurfaces thereby providing a 5-D representation of the mixing process. When operating in this single-feed semi-batch mode, the ERT system can clearly distinguish the higher conductivity feed plume. The ERT also images the subsequent mixing in the vessel after the semi-batch feed addition has stopped, thus additionally characterising the role of macro-mixing in achieving final homogeneity after a period of semi-batch operation. The results to be presented are extremely useful for the validation of CFD predictions of mixing behaviour.

Keywords: electrical resistance tomography, fluid mixing, stirred vessel, semi-batch

1. INTRODUCTION

Large scale precipitators (up to 20 m³ in volume) operated semi-batch wise are often used to manufacture solid products produced by mixing miscible liquids. Earlier studies involved continuous precipitators with over simplified models with only 3 or 4 zones combining macromixing and micromixing, Tavare (1). The quality of solid products is measured in terms of particle size, morphology and purity. The interactions of fluid mixing and precipitation reactions can be extraordinarily critical in producing solids suitable for on-going manufacturing requirements. Typically, these stirred vessels have little or no instrumentation and the requisite mixing is arrived at by trial and error. The complex concentration fields in 3-D need to be quantified and subsequently carefully controlled to produce a high quality material. The schematic situation is shown in the figure 1, where a complex concentration field in 3-D varies in space and time as the semi-batch stirred addition proceeds. Ultimate control of final solid quality almost certainly requires close control of this evolving complex space-time concentration field. Unfortunately, very little is understood about the fundamentals of fluid flow, mixing, supersaturation and nucleation, which together govern the overall solid formation and particle growth processes. The situation in figure 1 shows that, typically, because of the speed of the reaction relative to rates of fluid mixing, the fluid will be far from well mixed.

It is also most desirable to be able to interrogate the full volume in 3-D inside a typical single feed semi-batch reactor. In particular, it is extremely useful to be able to map out the conductivity distribution in space as this provides a strong indication of the extent of mixing and/or reaction. If the spatial concentration fields could also be measured in 3-D, this would provide a powerful new basis for control of chemical reaction rates in space, which would offer the capability to suppress by-product reactions by suitable control of concentration levels, their location and interaction. Electrical tomographic methods provide a means to obtain a 3-D scanning of the interior of the reactor space. The discrimination of spatial information can be of the order $O(10^3)$ with fast acquisition.

The recent and rapid development of tomographic techniques, as applied to the process industries, can be judged by two recent textbooks, Williams and Beck (2) and Chaouki *et al* (3). Electrical techniques being developed and applied at UMIST include electro-magnetic, Yu *et al* (4), capacitance, Dyakowski *et al* (5) and resistance tomography, Mann *et al* (6).

Earlier work has shown that an "8-level + 16-ring sensors" electrical resistance tomography (ERT) array could be applied at an industrial process vessel scale to measure salt concentration fields in 3-D during an unsteady tracer test, Stanley *et al* (7). Also it has been demonstrated that the pseudo-stationary distribution of gas hold-up could be pictorialised in 3-D for typical stirred vessel gas-liquid mixing, Holden *et al* (8). Subsequently, the UMIST/ITS ERT system was applied to demonstrate that the homogeneous single phase mixing created by different impeller types could be readily distinguished. In addition, further work showed how such an ERT system could be used to diagnose the types of pathological mixing symptoms likely to be associated with equipment malfunction or failure, Holden *et al* (9).

Most recently it has become evident that ERT can be configured to measure the pseudo-stationary solids distribution inside a stirred vessel as well as the solids distribution during the dynamic addition of a solids charge, Mann *et al* (10). Each of the aforementioned examples confirms that ERT does provide a powerful new means for direct experimental investigation of the rates of fluid mixing and reaction.

2. EXPERIMENTAL EQUIPMENT

The ERT experiments were carried out on a flat-bottomed polypropylene stirred tank of diameter $T = 1.43$ m, shown in figure 2. The liquid height, H , inside the tank is equal to the tank diameter providing a total volume of around 2,300 litres (2.3 m^3). Each of the four full-length baffles of width $T/10$ are attached to the vessel wall by a number of polypropylene brackets. All experiments used the six-blade Rushton Turbine, of diameter $D = T/3 = 0.477$ m, which was set to a clearance of $H/3$ above the base. The impeller itself is driven by a variable speed motor, which is able to provide speeds in the range of 75 to 250 rpm.

The vessel in figure 3 has been retro-fitted with a newly configured ERT system consisting of 16 vertical running sensor sections equally spaced around the vessel circumference. Also in view is the semi-batch feed line, the four baffles, impeller and impeller shaft. Each layer of the sensor 'rings' is equally axially spaced (16.5 cm apart) along the liquid height, H . The sensors themselves comprise of stainless steel plates 100 mm x 38 mm. The system makes use of an adjacent measurement protocol that provides 104 individual measurements per plane. The eight axial layers thus give rise to 832 interrogative measures of the liquid volume (which in the case of $H=T$ is 2.3 m^3). For experiments presented here, only

the top seven ERT sensor rings were operating within acceptable parameters. The ERT system operates to a spatial resolution of around 5%, that is, each individual tomogram (image of the vessels cross-section at a particular sensor ring location) consists of a 20 by 20 pixel array giving a total of some 400 spatial elements. Compared to the previously used Mk 1B-E (9) system, the new ITS P2000 system has an improved timewise resolution providing up to 24 individual tomograms per second (i.e. at video frame rates), ITS P2000 users manual (11).

3. SINGLE FEED SEMI-BATCH OPERATION OF A STIRRED VESSEL

The ERT system, operating with the top seven rings only, was used to monitor changes in conductivity during the single feed semi-batch addition of brine into a stirred vessel. The semi-batch feed, consisting of 40 litres of strong brine, was fed into the vessel over a period of 5 minutes in order to mimic conventional semi-batch operation.

The point at which the semi-batch feed is introduced into the vessel does have a strong influence on the rate of mixing as well as the observed mixing pattern as previously observed (10). It is sensible to add any feeds at a point in the vessel where there are high levels of local flow and turbulence, which should aid the mixing process, for example midway between the impeller shaft and a baffle edge. For all experiments reported here, the semi-batch feed was introduced at the liquid surface midway between the impeller shaft and vessel wall. The experiment used the Rushton disc turbine at a rotational speed of 75 rpm.

For semi-batch feed, the pixel values per frame (equivalent conductivity changes) are presented in figure 4. The green line on the figure represents the average recorded pixel value, the red is the maximum and blue the minimum. As expected, for times less than t_f , the average conductivity inside the vessel increases linearly indicating the 'constant' semi-batch feed addition. The maximum recorded conductivity (red line) increases quickly immediately after the semi-batch feed proceeds suggesting that a resultant feed plume may be detected. For times after t_f , the average conductivity inside the vessel seems to stay at a constant level. The maximum recorded conductivity however falls slightly after t_f indicating an increase in homogeneity inside the vessel which is caused by the continuing mixing.

As well as plotting the average pixel value per frame, as in figure 4, the ITS windows based software also offers the possibility to plot the conductivity profiles for each of the individual planes providing a higher 'information density' per frame. Figure 5 is such a representation. Like the previous conductivity profile, the green line represents the average-recorded pixel value for that plane, red the maximum and blue the minimum. The feed time, t_f , in this case 5 minutes is clearly marked on each of the eight plots as a dotted line.

The average conductivity profiles (green) for seven planes, P1 to P7 follow a similar trend and all have approximately the same peak value. The maximum-recorded conductivity profiles (red) are different, that is, the highest peak value occurs in P1. The value of this peak seems to fall along the depth of the vessel (P2 to P7) suggesting that for times before t_f the maximum recorded conductivities occur in the top half of the vessel. Perhaps a more relevant feature deducible from figure 5 is the range of measured conductivity values (i.e. the difference between the maximum and minimum recorded conductivity values) as this provides a real measure of non-homogeneity for any given plane and frame. For times less than t_f , it can clearly be seen that the range of measured values for P1 is the highest with P2, P3 and P4 about the same. Planes 5 through 7 all have a significantly lower range of

measured conductivity values. For times less than t_f , the ERT results have highlighted lower levels in homogeneity in the upper half of the vessel as compared to the lower half of the vessel which again suggests the presence of a distinct feed plume.

The presence of the feed plume is highlighted in figure 6, which shows both a 3-D variable opacity triple iso-surface representation as well as a pixel value distribution for time zero (just as the semi-batch feed is introduced into the vessel). On the 3-D image, the three variable opacity iso-surfaces are clearly marked. The first, iso-surface A, representing those few pixels with the highest conductivity value, is an opaque layer whose 'real' value is marked on the pixel distribution. Iso-surfaces B and C have progressively lower opacities, which are also marked on the pixel distribution. Because the ERT system was operating with seven out of eight sensor rings, there is a small volume of the vessel that is outside the sensors range. This volume is separated from the rest of the volume by a dotted line as seen at the bottom of the 3-D image in figure 6.

The presence of the feed plume for times less than t_f i.e. during the addition is also highlighted in figure 7. The images on the extreme right of the figure are generated from the raw ERT data. The first three, corresponding to times 0, 1 and 3 minutes, are imaged as 3-D variable opacity triple iso-surface representations. In these images each of the three variable opacity iso-surfaces each corresponds to a particular conductivity value. The last two, corresponding to times 5 and 8 minutes, are also generated from raw ERT data but are represented as seven slices, each corresponding to one of seven operating ERT rings. After the semi-batch feed has stopped, for times greater than t_f , a feed plume is no longer observed.

Located in the centre of figure 7 are the pixel distributions that, as mentioned earlier, provide a direct indication of the non-homogeneity within the vessel. The first three, each with a relatively wide distribution (less homogeneous), highlight the pixel distributions 'migration' to the right (higher conducting) for times less than the feed time, t_f .

After the semi-batch feed ceases, the observed 'migration' stops. These two plots, for times of 5 and 8 minutes, both have a significantly narrower distribution (more homogeneous) than the previous three, times 0, 1 and 3 minutes. The pixel distribution for 8 minutes, which represents the final state of the vessel, is extremely narrow (much more homogeneous) indicating the subsequent 'mixing in' of the semi-batch feed is becoming complete.

4. CONCLUSIONS

- A newly refurbished 8-plane 16-sensor ring ERT system can produce $O(10^3)$ data points inside the 3-D fluid space of a typical cylindrical stirred vessel. Interpolation between the 10^3 points from simple linear back projection can produce augmented reality images of fluid mixing processes. Such images are created by solid-body iso-surface or sliced images that, with the use of colour to denote conductivity, give rise to a double-augmentation of the interior behaviour producing a four or five dimensional format.
- An application to the semi-batch feed addition of strong brine has been presented, which can readily highlight the conductivity profile within the vessel during the semi-batch addition. Two main regions have been highlighted, reflecting the conductivity distribution during and after the semi-batch feed time.
- The pixel distribution plots and 3-D ERT images provide a powerful measure of the homogeneity within the vessel, which has been used to investigate the nature of the feed

plume induced by the semi-batch feed. The nature of this feed plume varies from low conducting to high(er) conducting depending on the time during the semi-batch addition.

5. NOMENCLATURE

t_f	Feed time	[s]
V_{feed}	Volume of semi-batch feed	[m ³]
V_{tank}	Volume of tank	[m ³]

6. ACKNOWLEDGEMENTS

The authors gratefully acknowledge support from the EPSRC (Total Technology Studentship) and additional financial support from ITS (Industrial Tomography Systems), Manchester, England.

7. REFERENCES

1. Tavaré, N. S., Mixing, reaction and precipitation: an interplay in continuous crystallizers with unpremixed feeds, *10th European conference on mixing*, pp 395-405, 2000.
2. Williams R.A. and Beck M.S. (Editors), *Process Tomography: Principles, Techniques and Applications*, Butterworth-Heinemann Ltd, Oxford, UK, 1995.
3. Chaouki, J., Lavachi, F. and Dudokovics, M.P., *Non-invasive Monitoring of Multi-phase Flows*, Elsevier, Amsterdam, 1997.
4. Yu Z.Z., Peyton A.J., Beck M.S., Conway W.F. and Xu L.A., Imaging systems based on electromagnetic tomography (EMT), *Electronic Letters*, 29(7), 1993.
5. Dyakowski T., Wang S.J., Geldart D. and Beck M.S., Tomographic studies of flow patterns within a circulating fluidised bed, *Chem. Eng. Comm.*, **175**, 117-130, 1999.
6. Mann R., Dickin F.J., Wang M., Dyakowski T., Williams R.A., Edwards R.B., Forrest A.E., Application of Electrical Resistance Tomography to Interrogate Mixing Processes at Plant Scale, *Chem. Eng. Sci.*, **52**(13), 2087-2097, 1997.
7. Stanley, S.J., Wabo, E., Mann, R. and Primrose, K., Dual-Validation of Miscible Liquid Mixing in a Stirred Vessel Imaged by Electrical Resistance Tomography, *2nd world congress process tomography*, Hannover, Germany, pp 151-158, 2001.
8. Holden P.J., Mann R., Wang M., Dickin F.J. and Edwards R.B., Imaging Stirred-Vessel Macromixing Using Electrical resistance Tomography, *AIChE Journal*, **44**(4), 780-790, 1998.
9. Holden P.J., Wang M., Mann R., Dickin F.J. and Edwards R.B., On Detecting Mixing Pathologies Inside a Stirred Vessel Using Electrical Resistance Tomography (ERT), *Trans IChemE*, **77**(A), 709-712, 1999.
10. Mann R., Stanley, S.J., Vlaev, D., Wabo, E., and Primrose, K., Augmented-reality visualisation of fluid mixing in stirred chemical reactors using electrical resistance tomography (ERT), *SPIE Journal of Electronic Imaging*, 620-629, 2001
11. ITS P2000 users manual, Industrial Tomography Systems Ltd., 47 Newton Street Manchester, UK, M1 1FT, (www.itoms.com).

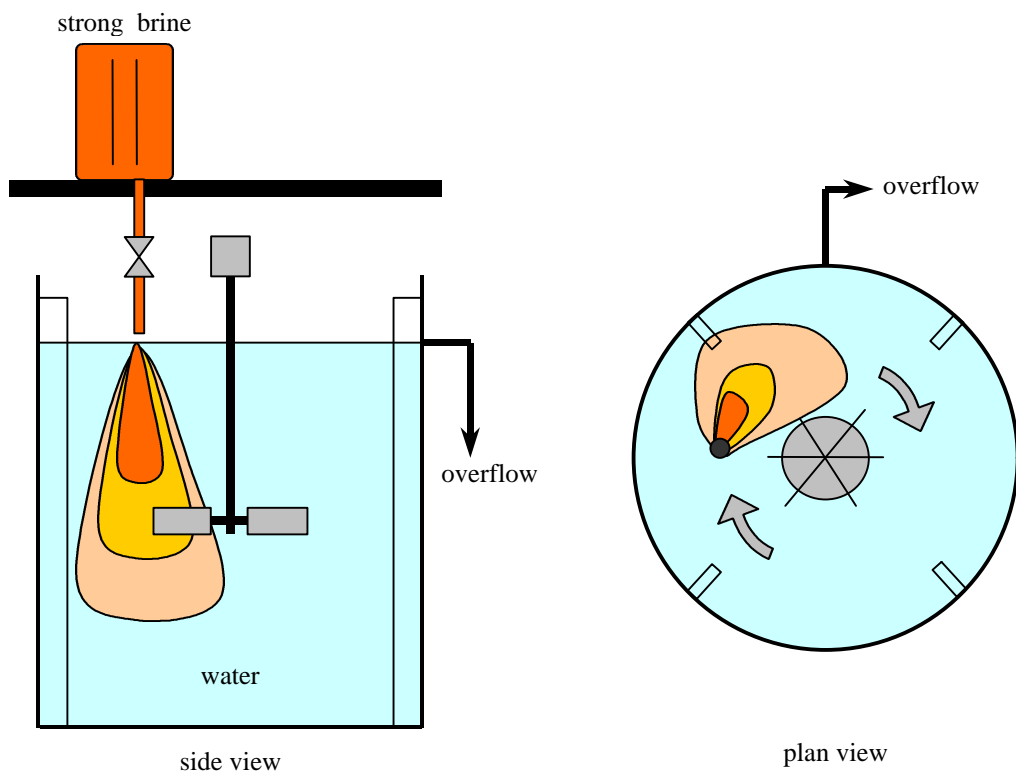


Figure 1: Single-plume semi-batch addition experimental layout

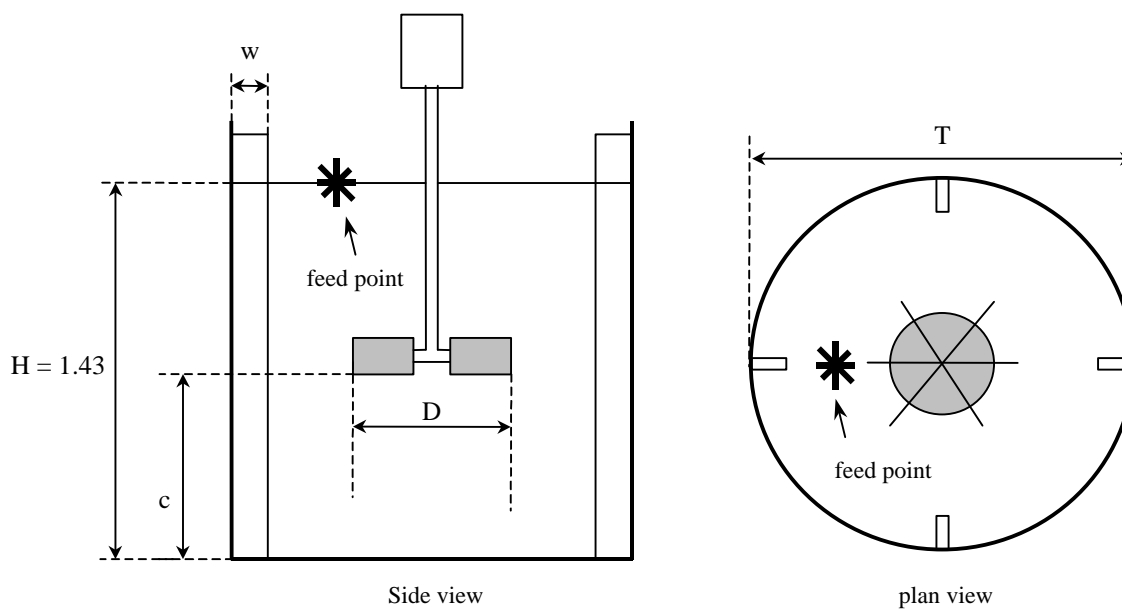


Figure 2: Schematic representation of stirred vessel

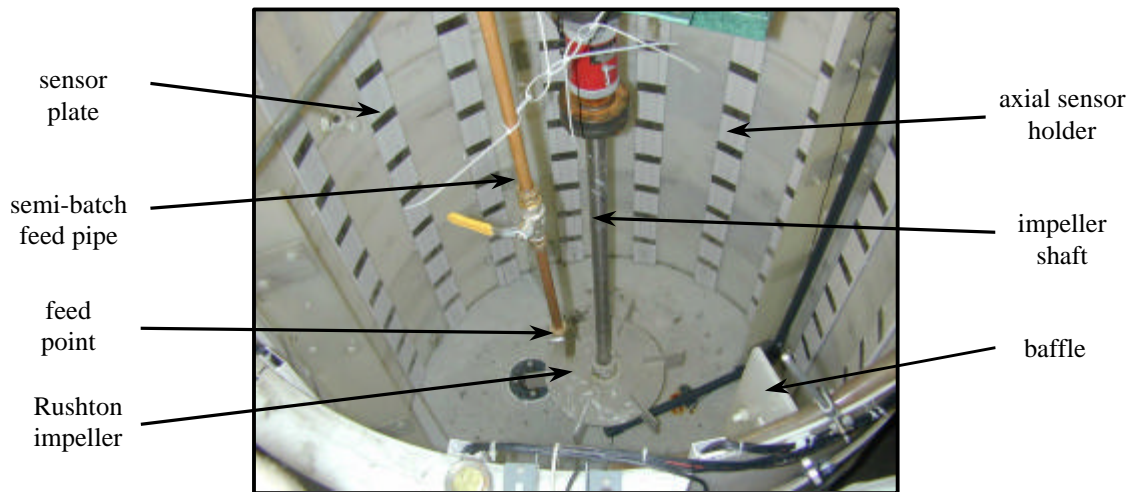


Figure 3: Photograph of the newly refurbished eight plane, sixteen electrode arrangement

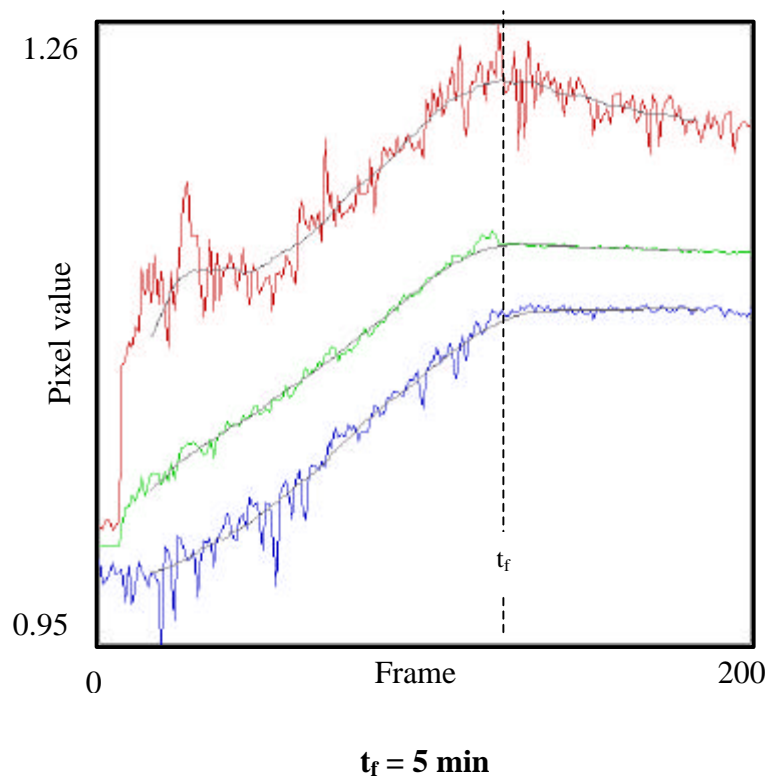


Figure 4: Conductivity variations per frame during the semi-batch addition of strong brine, agitator at 75 rpm

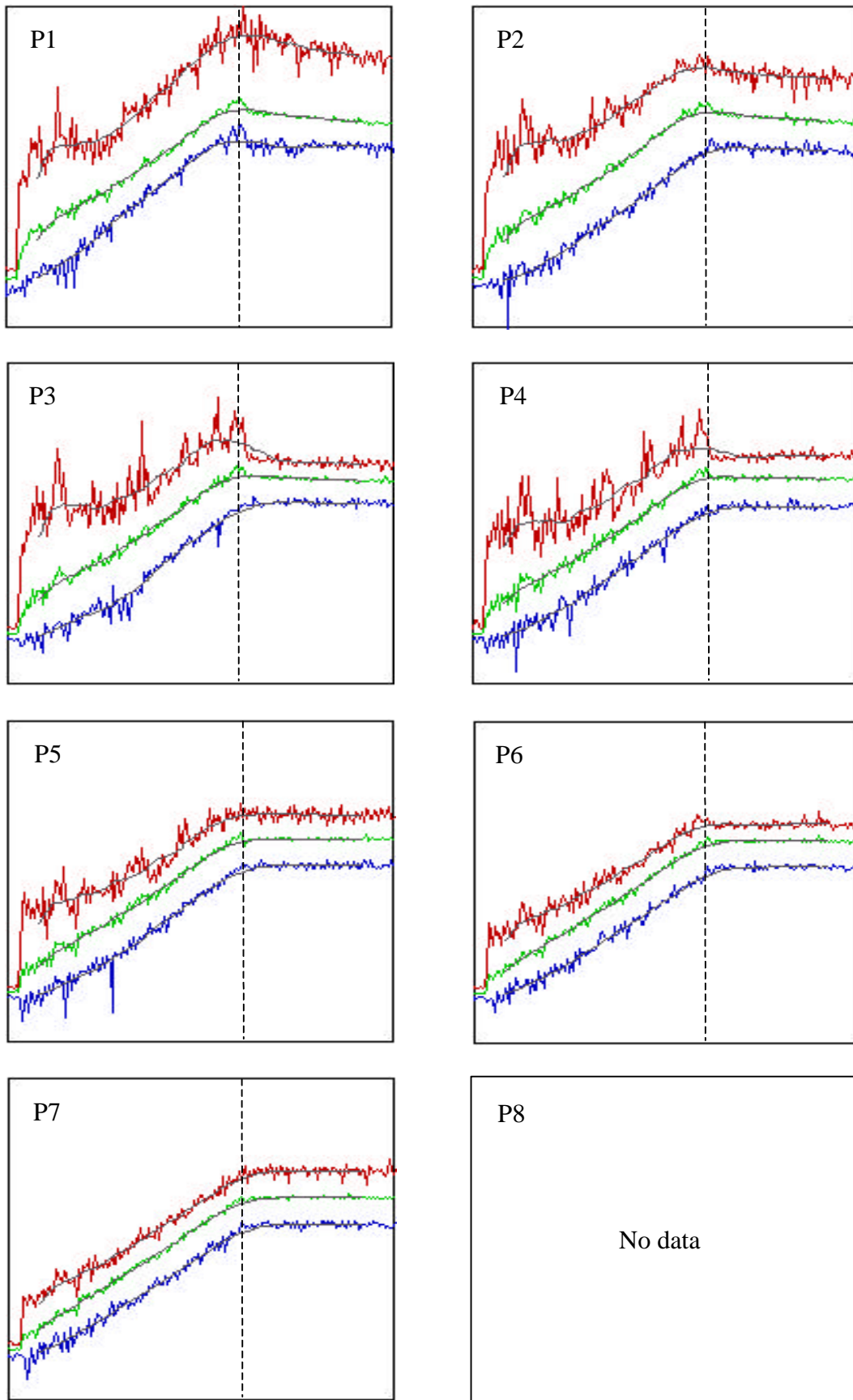


Figure 5: plane by plane conductivity profiles during the semi-batch addition of strong brine

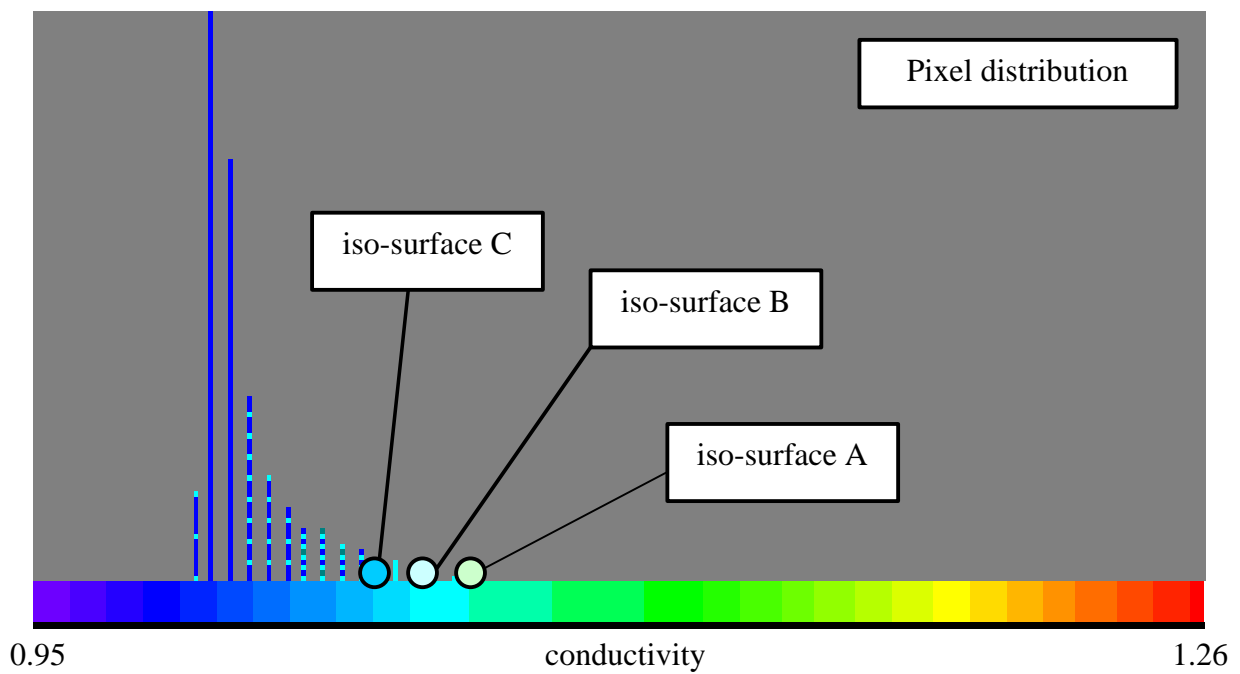
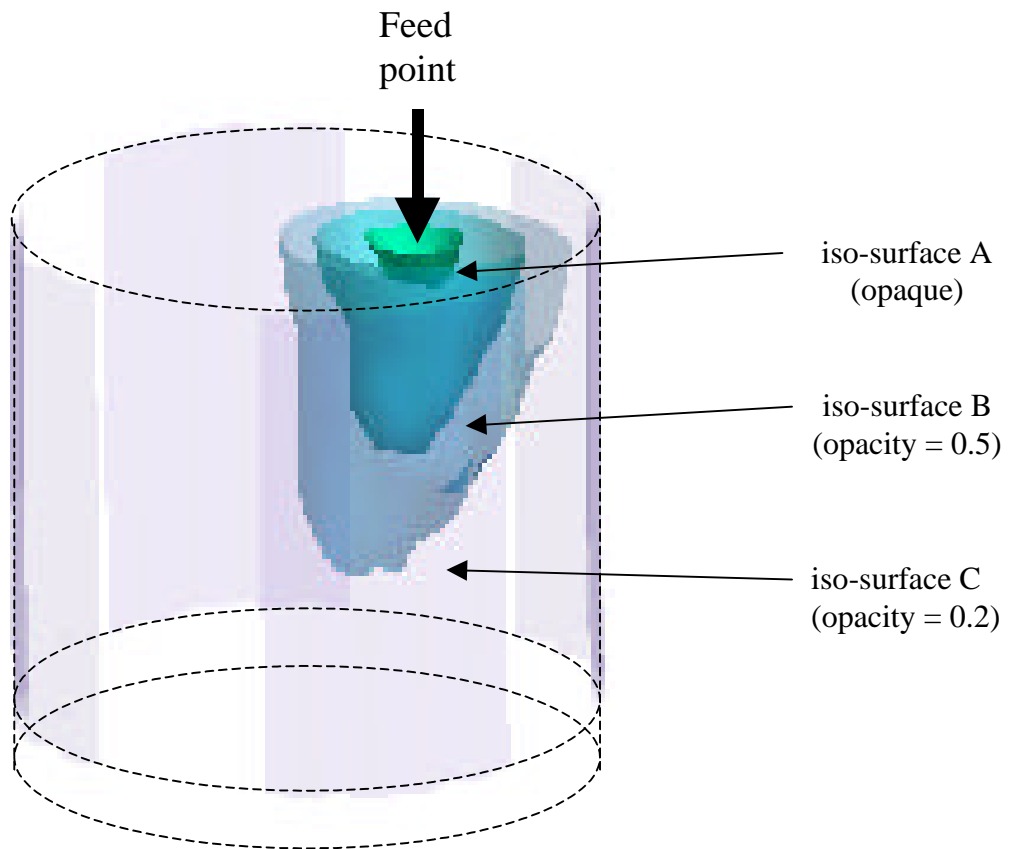


Figure 6: 3-D variable opacity triple iso-surface representation of ERT data

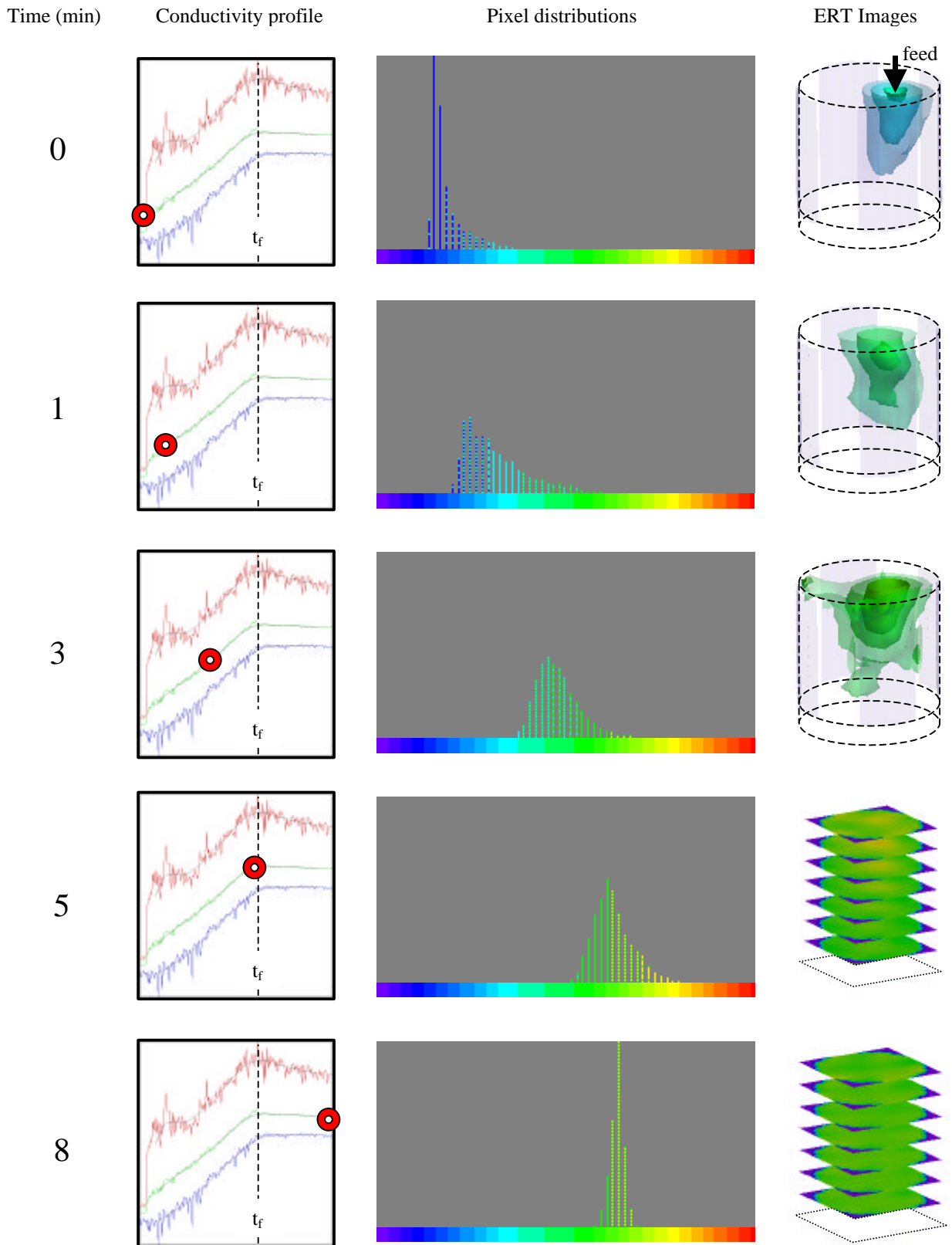


Figure 7: ‘Dynamics’ in time of pixel distribution and 3-D ERT images during semi-batch feed addition